Construction and Building Materials 53 (2014) 190–202

Contents lists available at ScienceDirect

Construction and Building Materials

journal homepage: www.elsevier.com/locate/conbuildmat

Study of nopal mucilage and marine brown algae extract as viscosity-enhancing admixtures for cement based materials

F.M. León-Martínez [a,*], P.F. de J. Cano-Barrita [a], L. Lagunez-Rivera [a], L. Medina-Torres [b]

[a] Instituto Politécnico Nacional-CIIDIR Unidad Oaxaca, Hornos No. 1003, Sta. Cruz Xoxocotlán, C.P. 71230 Oaxaca, Mexico
[b] Universidad Nacional Autónoma de México, Facultad de Química, Conjunto E, L213, C.P. 04510, D.F., Mexico

HIGHLIGHTS

- Two new bio-polymers are proposed as alternative viscosity-enhancing admixtures for cement-based materials.
- Nopal mucilage and marine brown algae extract dispersions showed a shear-thinning behavior.
- The Herschel–Bulkley yield-stress increased with increasing brown algae extract concentration in cement based materials.
- Stable, cohesive and homogeneous SCC mixtures can be produced using both new VEAs.

ARTICLE INFO

Article history:
Received 21 June 2013
Received in revised form 10 November 2013
Accepted 20 November 2013
Available online 20 December 2013

Keywords:
Nopal mucilage
Brown algae extract
Viscosity-enhancing admixture
Yield-stress
Self-consolidating concrete

ABSTRACT

Viscosity-enhancing admixtures (VEAs) are required in the production of self-consolidating concrete (SCC). This paper presents the rheological properties in rotational and oscillatory shear tests of cement pastes and mortars with a w/c ratio of 0.50, containing nopal mucilage and marine brown algae extract, which are proposed as two new VEAs. For comparison purposes, a commercial VEA based on welan gum was used. In addition, preliminary SCC mixtures were prepared using the proposed and the commercial VEA. The slump flow, J-ring, L-box, V-funnel and static segregation column were used to evaluate the SCC fresh state properties. The results indicated that the new VEAs produced a significant increase on the shear viscosity and the yield-stress of pastes, mortars and SCC, which increased with increasing concentration and depending on their molecular nature. This was more noticeable in the mixes containing brown algae extract, which may be related to chains' entanglement and gel-network formation. Cement pastes and mortars containing the proposed VEAs exhibited a solid-like behavior at short values of strain amplitude (<1%). The proposed VEAs produced some stable and homogeneous SCC mixtures in comparison with the commercial VEA based in welan gum.

1. Introduction

Concrete based on Portland cement is the most widely used construction material in the world, and its production follows a trend of growth. In 2011, the world production of Portland cement reached 2.8 $\times 10^9$ tonnes and is expected to increase around 4×10^9 tonnes for the 2050 [1]. About 15% of the total concrete production contains chemical admixtures [2], which are chemicals added to concrete, mortar or grout at the time of mixing to modify their properties, either in fresh or hardened state [3].

Self-consolidating concrete (SCC) is a highly flowable and stable concrete that flows under its own weight, and can be compacted without any external consolidation [4,5]. SCC allows increased productivity levels as it shortens construction time and reduces construction costs. It also improves the working environment, the quality of concrete under difficult casting conditions, and the surface quality [6].

Modern production of SCC requires the use of chemical admixtures such as superplasticizers (SPs) and viscosity-enhancing admixtures (VEAs) used to achieve high flowability and high resistance to segregation of concrete, respectively [7]. SPs are linear

Abbreviations: ALG, marine brown algae extract; ALGD, marine brown algae extract dispersion; ATR, attenuated total reflection; BMS, ball-measuring system; C, Portland cement; CAgg, coarse aggregate; CM_0, control cement mortar; CP_0, control cement paste; CSH, calcium-silicate hydrate; FAgg, fine aggregate; FTIR, Fourier transform infrared spectroscopy; LVE, linear viscoelastic; M, cement mortar; MUC, nopal mucilage; MUCD, nopal mucilage dispersion; Na-alginate, sodium alginate; Na-AlginateD, sodium alginate dispersion; P, cement paste; PVC, poly (vinyl-chloride); RM, reference mortar; RP, reference paste; RSCC, reference self-consolidating concrete; SCC, self-consolidating concrete; SP, superplasticizer; VEA, viscosity-enhancing admixture; W, water.

* Corresponding author. Tel.: +52 951 51 7 06 10x82713.
E-mail addresses: leon.frk@gmail.com (F.M. León-Martínez), pcano@ipn.mx (P.F. de J. Cano-Barrita), llagunez@ipn.mx (L. Lagunez-Rivera), luismt@unam.mx (L. Medina-Torres).

0950-0618/$ - see front matter © 2013 Elsevier Ltd. All rights reserved.
http://dx.doi.org/10.1016/j.conbuildmat.2013.11.068

polymers containing sulfonic groups attached at regular intervals to the polymer backbone. Most formulations belong to one of the following groups: sulfonated melamine–formaldehyde condensates, sulfonated naphthalene-formaldehyde condensates, modified ligno sulfonates and polycarboxylate derivates [8].

While resistance to segregation can be achieved by using a large amount of fine materials, the preferred approach is to use VEAs [5]. These are water-soluble polymers that increase the viscosity and cohesion of cement-based materials [6,9]. The common viscosity-enhancing admixtures used in concrete production include microbial polysaccharides such as welan gum, cellusose derivates (methyl cellusose and cellulose ethers), alginates, acrylic-based polymers, polyethylene oxides and mineral materials such as colloidal silica and fine carbonate fillers, among others [5–10]. The main disadvantage of the commercial VEAs is their high cost, which increases the overall cost of the SCC and makes it non-competitive with respect to ordinary concrete.

The use of admixtures in the concrete industry is increasing, especially the use of bio-admixtures, which are functional molecules used to modify material properties. The global expenditure of bio-admixtures in the year 2000 was estimated at US $ 2×10^9 [2]. It is evident that the cost of SCC will be reduced if admixtures are cheaper and more readily available. Some alternatives to the commercial VEAs are polysaccharides from nopal mucilage and marine brown algae.

Nopal mucilage, from the *Opuntia* gender, has been used as an additive to improve the durability of lime-based mortars [11] and to improve the Portland cement concrete [12]. It also inhibits aluminum and steel corrosion [13–15] and increases the plasticity of mortars and reduces their permeability [16]. A preliminary study using the mini cone test [12] has demonstrated the potential use of nopal mucilage as VEA for SCC. On the other hand, alginates from brown algae have been used as a bonding agent in composites, increasing compressive strength without any effect on flexural strength [17] and they have been suggested as potential VEA for concrete [6].

Therefore, in this research the rheological behavior of cement pastes and mortars containing nopal mucilage or brown algae extract was studied and compared to a commercial VEA. These viscosity-enhancing admixtures were also used in trial mixtures to demonstrate their suitability to produce stable SCC.

2. Materials and method

2.1. Materials

2.1.1. Cement aggregates and water

Ordinary Portland cement 30 R RS BRA with a Blaine fineness of 318.2 $m^2\ kg^{-1}$ was used in all the mixtures. Table 1 presents its chemical properties. Silica sand with specific gravity of 2.61, water absorption of 0.30% and fineness modulus of 2.91 was used to prepare the mortars for the rheological tests.

Table 1
Chemical analysis of ordinary Portland cement 30 R RS BRA, by mass percent.

Composition	%
Al_2O_3	3.69
CaO	58.77
Fe_2O_3	3.97
K_2O	0.31
MgO	1.58
MnO	0.10
Na_2O	0.18
P_2O_5	0.10
SiO_2	18.77
TiO_2	0.17
Loss on ignition	5.39

For the SCC mixtures, river gravel with 9.5 mm maximum size was used as coarse aggregate, having water absorption of 1.90% and a specific gravity of 2.48. The fine aggregate was river sand having a fineness modulus of 2.96, water absorption of 2.80% and a specific gravity of 2.68. The particle size distributions of both sands are presented in Table 2.

Distilled water was used to prepare the VEAs dispersions, cement pastes and mortars. Tap water was used in the SCCs mixtures.

2.1.2. Viscosity enhancing admixtures (VEAs)

2.1.2.1. Nopal mucilage. *Opuntia ficus-indica* cladodes were used to extract the mucilage (MUC). These cladodes had a moisture content of 93% (wet basis). An aqueous extraction with heating was used (Fig. 1-A). The cladodes were diced into thin slices with a thickness of 2 ± 0.2 mm. Then the slices were weighed and put into an aluminum container and distilled water was added to obtain a mix with a water-to-raw material ratio by weight of 2. The mucilage was extracted at a temperature of 60 ± 5 °C for a period of 3 h with manual agitation approximately every 10 min. The extracted mucilage was then separated from large particles by decantation and then filtered using a sieve No. 100 (150 μm). It was kept refrigerated until use (Fig. 1-C). A refractometer (Westover, model RHB-32ATC) was used to determine its concentration in degrees Brix. The solid content in the extract used for cement pastes and mortars was 8.70 ± 0.30 g L^{-1}, whereas the extract used for the SCC mixtures had a solid content of 7.33 ± 0.23 g L^{-1}.

2.1.2.2. Marine brown algae extract. A concentrated extract of marine brown algae (*Macrocystis pyrifera*) used in the industry as a binder in the production of pellets and extruded foods was used in our experiments as raw material (ALG). This ALG is a semi-pasty dispersion with a high content of polysaccharides, minerals and proteins. It was used in this study because of its lower cost compared to that of high purity alginate salts (Fig. 1-B and 1-C). In addition, sodium alginate (ACS grade) was used to prepare aqueous dispersions at concentrations of 5 g L^{-1}, 10 g L^{-1} and 20 g L^{-1} in order to compare its viscous behavior with the ALG.

Table 2
Particle size distributions of silica sand and river sand.

Sieve size (mm)	Silica sand (F.M. = 2.92) (% passing)	River sand (F.M. = 2.96) (% passing)
4.75	100	97.90
2.38	100	82.90
1.20	92.60	63.05
0.599	15.28	40.01
0.297	0.34	16.66
0.152	0.11	3.38
0.075	0.05	1.01
Pan	0	0

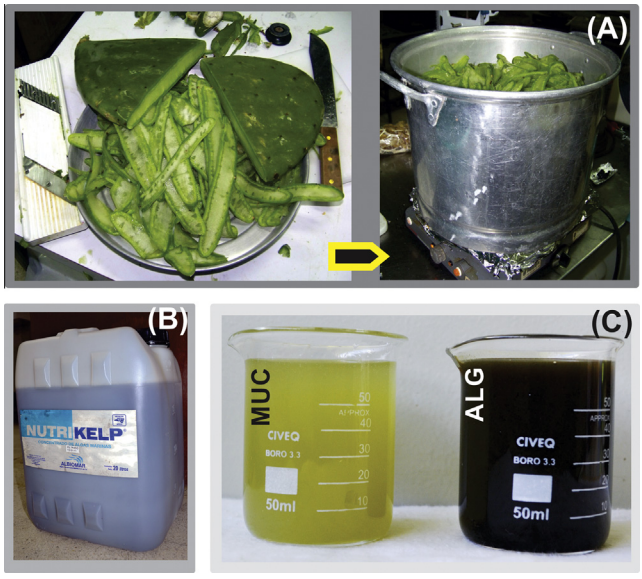

Fig. 1. Nopal mucilage extraction process (A); concentrated ALG (B); MUC and ALG dispersions (C).

The proximate analysis of the brown algae extract given by the supplier, as well as the total solid content, suspended solids, density (at 12 °C), °Brix, pH and moisture content (wet basis) determined in laboratory are presented in Table 3.

2.1.2.3. Commercial VEA. In order to compare the performance of our proposed VEAs, a commercial one based on welan gum with a density of 1.23 kg L^{-1} and total solid content of 50% was used.

2.1.3. Superplasticizer

A polycarboxylate based SP with a density of 1.07 ± 0.01 kg L^{-1} and total solid content of 30% was used in just all the mixtures.

2.2. Method

2.2.1. Fourier transform infrared spectroscopy measurements

The infrared spectra of powdered sodium alginate (ACS grade), ALG and MUC (both oven dried at 105 °C) were performed on a Thermo Scientific spectrometer model Nicolet 6700 with an attenuated total reflection (ATR) accessory featuring a diamond crystal. The spectral scanning was taken in the wavelengths region between 4000–650 cm^{-1} at a resolution of 4 cm^{-1}. The total number of scans was 64.

2.2.2. Mix proportions

The mix proportions used to prepare the pastes and mortars (Table 4) were based on the results of previous work undertaken to develop a SCC with regional materials (Cano-Barrita et al., 2009[1]). Dispersions at different concentrations of MUC and ALG were used to replace the mixing water. The concentration of each VEA was calculated with respect to cement weight (%w), taking into account their solids content. The corresponding concentration of the dispersions in w/v is also presented in Table 4. For MUC solutions two levels of concentration were used and for ALG dispersions three levels were selected.

Control cement paste (CP_0) and mortar (CM_0) were prepared without any SP and VEA. The sand-to-cement ratio by weight used in mortars was 2.2.

2.2.3. Mixing procedure

The cement pastes and mortars were prepared at room temperature (24 ± 1 °C) using a planetary motion mixer (Hamilton Beach, model 63221).

To prepare the pastes and mortars with the proposed VEAs (MUC and ALG), half of the total volume of the respective dispersion was used to disperse the SP. For the reference paste (RP) and reference mortar (RM), the total mixing water was separated into two equal parts. The first part was used to disperse the SP and the second part was used to disperse the commercial VEA.

To prepare the mortars, the sand was poured into the mixer and the absorption water was added and mixed at low speed (11.77 ± 0.17 rad s^{-1}) for 60 s. The cement was then added and mixed for other 60 s. The speed of the mixer was immediately changed to 16.35 ± 0.23 rad s^{-1} and the first part of the mixing water was incorporated. The mixing continued for other 120 s. Then, the mixer was stopped and the mortar was homogenized by hand for 45 s. After this, the second part of the mixing water was added; the mixer was restarted at a speed of 16.35 rad s^{-1} and mixed for additional 280 s.

The mixing procedure for the cement pastes was similar to that used to prepare the mortars. In this case, the cement and the first part of mixing water were incorporated from the beginning.

2.2.4. Rheological characterization of nopal mucilage and marine brown algae extract

Rheological tests were performed with a controlled-stress rheometer (Anton Paar, model Physica MCR 301). The data analysis was performed using the software Rheoplus/32 version 3.00.

The rheological behavior in steady-shear flow was investigated for dispersions with different concentrations of MUC and ALG. In this case a concentric cylinder of double-gap (Model DG26.7-SN21085) was used. The internal and external gaps are 0.418 mm and 0.464 mm, respectively. The temperature was kept constant at 25 ± 0.2 °C by a Peltier system connected to a Julabo F-25 water bath. The shear rate was varied from 0.01–600 s^{-1}.

2.2.5. Rheological tests in cement pastes and mortars

Two types of rheological tests were used to determine the rheological properties of each mixture. The first one was an oscillatory test to determine the viscoelastic properties and the second one was a continuous rotational test to obtain the flow curves.

The Anton Paar ball measuring system (BMS) was used to perform the rheological tests. It is intended to measure semisolid dispersions containing particles up to 5 mm in diameter [18]. For cement pastes, the diameter of the ball used was 8 mm, and for mortars the diameter was 12 mm. The temperature of the pastes and mortars was kept constant at 25 ± 0.2 °C by a re-circulating bath (Julabo F-25).

[1] Unpublished technical report.

Table 3
Proximate analysis of the brown algae extract and other physicochemical properties.

Parameter[a]		Parameter[b]	
Moisture content	90% max	Moisture content (wet basis %)	89.58 ± 0.091
Ash	4% max	Total solids content (g L^{-1})	109.85 ± 0.070
Crude fiber	1% min	Total solids suspended g L^{-1})	46.36 ± 4.412
Proteins	3.5% min	Density at 12 °C (kg L^{-1})	1.054 ± 0.0025
Organic matter	7% min	Degrees Brix (°Bx)	10.5
Total carbohydrate	5% min	Ash (mass %)	4.61
pH	6.5 min 7.0 max	pH	5.74

[a] Data provided by supplier (mass percentage).
[b] Data obtained in laboratory.

2.2.5.1. Oscillatory-shear tests. Immediately after mixing, approximately 500 mL of each mixture were poured into the container of the ball measuring system. The sample was allowed to rest for 125 s to ensure thermal equilibrium. An amplitude sweep test was conducted, applying incremental shear strain from 0.01% to 100% at an angular frequency of 10 rad s^{-1}.

2.2.5.2. Rotational-shear tests. Before starting the steady shear test, each one of the samples was homogenized using a shear rate of 50 s^{-1} for 60 s and left at rest for 30 s. This was done to eliminate the deformation history and to establish a reproducible initial state. The shear rate was ramped from 0.1–50 s^{-1} in a logarithmic form. The range used was based on the results obtained by Schatzmann et al. [19], who obtained rheological data for the low and medium range of shear rates. The SP dosage was at the saturation point (Fig. 2), which was obtained using mini-cone tests [20].

2.2.6. Preliminary SCC incorporating the proposed VEAs (MUC and ALG)

Based on previous work by the authors (Cano-Barrita et al., 2009[1]), six SCC mixtures were prepared, including a reference SCC containing a commercial VEA and five with the proposed VEAs (MUC and ALG). Details of the mixtures are presented in Table 5.

The mixing procedure for the SCC mixtures consisted of homogenizing the fine and coarse aggregate with half of the mixing water for approximately 120 s. Then, the cement was added and mixing continued for other 120 s. After that, the SP diluted in 1 L of mixing water was incorporated. The mixing continued for about 180 s. Finally, the remaining water was added and the concrete was mixed for 180 s. The commercial and the proposed VEAs were dispersed in the remaining mixing water. The temperature, air content and unit weight were determined in the fresh concrete.

The tests carried out to evaluate the filling ability, passing ability and the stability of the SCC mixtures were the slump flow specified in ASTM C1611/C1611M [21], the J-ring test according to the ASTM C1621/C1621M [22], the L-box, the V-funnel [23] and the column segregation test. The column was constructed using three sections of PVC pipes measuring 110 mm in diameter. The top and bottom sections were 165 mm in height, and the middle section was 330 mm in height. Concrete was poured into the column and left undisturbed for 15 min and then concrete in the top and bottom sections were collected and washed over a sieve No. 4 (4.75 mm). The retained coarse aggregate was weighted in saturated surface-dry condition. The percent static segregation was calculated using the equation reported by the ACI committee 238 given in 238.1R-08 [23].

3. Results and discussion

3.1. FTIR spectra analysis

The FTIR spectra of sodium alginate (Na-alginate), ALG and MUC are presented in Fig. 3. The spectrum of Na-alginate showed bands around 3317, 1595 and 1408 cm^{-1} which are due to the stretching vibrations of –OH, –COO (asymmetric) and –COO (symmetric) groups, respectively. The small bands observed around 2940 cm^{-1} were assigned to asymmetric and symmetric stretching vibrations of aliphatic C–H. Bands at 1035 and 945 cm^{-1} were attributed to the C–O–C stretching vibration with contributions from C–C–H and C–O–H deformation. The band at 867 cm^{-1} could due to vibration of its Na–O bond. This spectrum is in agreement

Table 4
Proportions of solid particles and concentrations of VEAs in the cement pastes and mortars.

	Mixture	w/c[a] (–)	s/c[a] (–)	SP	VEA	
				(%w)[b]	(%w)[b]	(g L^{-1})[c]
Cement pastes	P + ALG	0.50	0	0.321	0.125	2.5
		0.50	0	0.321	0.250	5.0
		0.50	0	0.321	0.500	10.0
	P + MUC	0.50	0	0.321	0.250	5.0
		0.50	0	0.321	0.435	8.7
	CP_0	0.50	0	0	0	0
	RP	0.50	0	0.321	0.065	1.3
	P-VEA[d]	0.50	0	0.321	0	0
Mortars	M + ALG	0.50	2.158	0.321	0.125	2.5
		0.50	2.158	0.321	0.250	5.0
		0.50	2.158	0.321	0.500	10.0
	M + MUC	0.50	2.158	0.321	0.250	5.0
		0.50	2.158	0.321	0.435	8.7
	CM_0	0.50	2.158	0	0	0
	RM	0.50	2.158	0.321	0.065	1.3

[a] w/c = water to cement ratio and s/c = sand to cement ratio.
[b] %w is percentage in weight of dry solids of each admixture with respect to cement weight.
[c] Concentration given by the weight of dry solids with respect to the total volume of aqueous dispersion.
[d] Cement paste without any VEA but with SP.

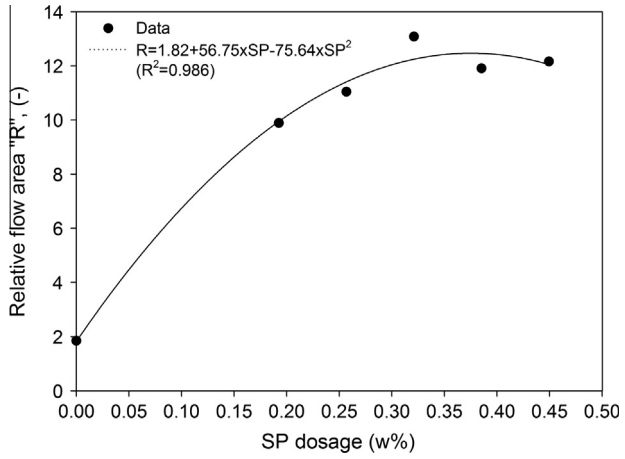

Fig. 2. Relative flow area against SP dosage for a cement paste with a w/c ratio of 0.50 and 22 °C.

with the literature. In comparison, ALG showed a broad band at 3273 cm^{-1} for its hydrogen bonded –OH group. Also, asymmetric and symmetric stretching of the carboxyl group were observed with higher intensity than the Na-alginate. However, the intensity of the band attributed to the C–O–C stretching vibration (~1029 cm^{-1}) was lower. This could be explained by the thermal decomposition of polysaccharides, which produces a reduction in the number of C–O–C bonds in the sample, and as a result the intensity decreases. C–N stretching vibration of aliphatic amines, from the amino acids in proteins, was observed in the region of 1271–1020 cm^{-1}. N–H stretching and bending vibrations were overlapped by the hydroxyl and carboxyl groups. Bands from 939–665 cm^{-1} corresponding to N–H wagging of primary and secondary amine were observed. The spectrum of MUC showed a band at 3273 cm^{-1} that corresponds to –OH stretching frequencies. The bands around 1316–1032 cm^{-1} were assigned to C–O–C with contributions of C–O–H and C–C–H stretching vibrations. Asymmetric CH_2 stretching vibration occurred at about 2918 cm^{-1} and symmetric CH_2 stretching absorption occurred at about 2849 cm^{-1}. The band around 1593 cm^{-1} was assigned to asymmetric –COO stretching vibration and the band around 1393 cm^{-1} to symmetric –COO stretching. A small band at 1515 cm^{-1} could be due to the contribution of C–N stretching and N–H bending vibration. However, N–H wagging from primary and secondary amines at 910–665 cm^{-1} and bending vibration of N–H group at 1600 cm^{-1} were not observed [16]. Therefore, the presence of a protein fraction in MUC is not clear and it is possible that the content of this fraction is marginal. These spectra confirm that for MUC the main functional groups are carbonyl, carboxyl and hydroxyl. The carboxyl group is present in uronic acids.

3.2. Rheological characterization of nopal mucilage and brown algae extract

Fig. 4 shows typical viscosity curves against shear rate for dispersions of MUC, ALG and pure Na-alginate at different concentrations (w/v) and at 25 °C. The fitting of experimental data to the indicated rheological models is given in Table 6. It is observed that all the dispersions exhibited a non-Newtonian behavior, where the shear viscosity decreased with increasing shear rate. This behavior is known as 'shear-thinning', which is dictated by the parameter

Table 5
SCC mixture proportions for 1 m^3.

Mixture	w/c Ratio (–)	C (kg m^{-3})	W (kg m^{-3})	CAgg	FAgg (kg m^{-3})	SP (%w)[a]	VEA (%w)[a]	Type of VEA
RSCC	0.51	408	208	711	928	0.321	0.065	Welan gum
SCC1	0.51	408	208	711	928	0.321	0.250	Nopal mucilage
SCC2	0.51	408	208	711	928	0.257	0.374	Nopal mucilage
SCC3	0.51	408	208	711	928	0.321	0.250	Algae extract
SCC4	0.51	408	208	711	928	0.276	0.250	Algae extract
SCC5	0.51	408	208	711	928	0.321	0.500	Algae extract

[a] %w is percentage in weight of dry solids of each admixture with respect to cement weight.

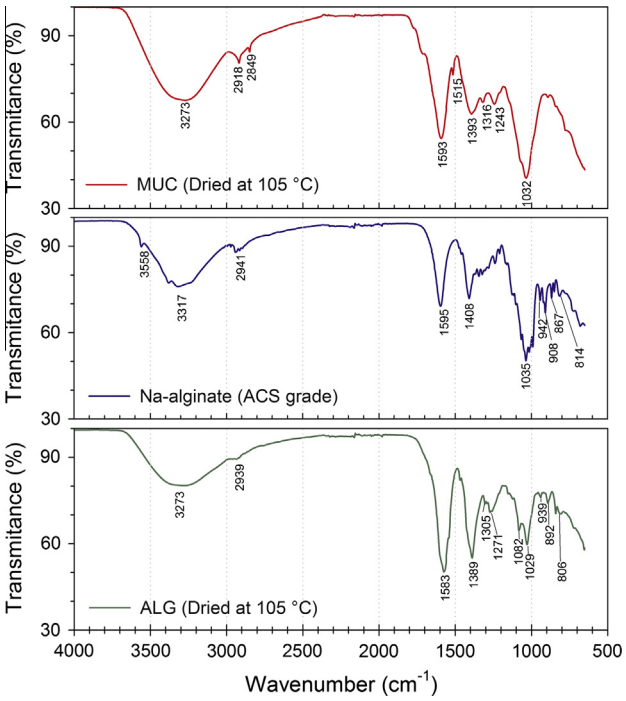

Fig. 3. FTIR spectra of Na-alginate, ALG and MUC.

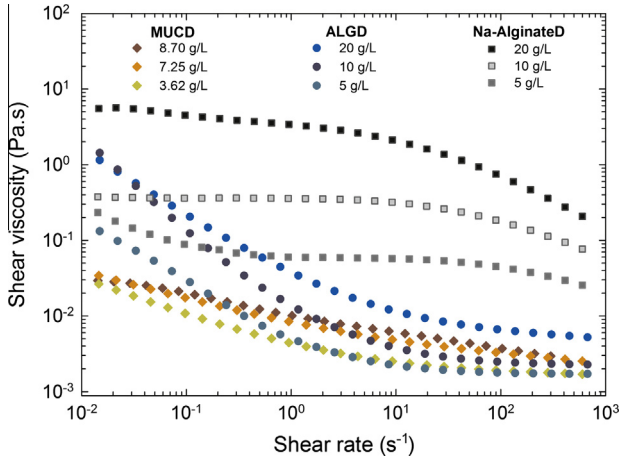

Fig. 4. Viscosity curves for proposed VEAs dispersions at 25 °C.

$n < 1$ in the Ostwald and Sisko models and $m > 0$ in the Cross model [18,24].

In the range of shear rate between 0.01–1 s^{-1}, the ALGD at lower concentration than MUCD had higher values of viscosity. This effect could be due to the high concentration of suspended solids in the algae extract and by the fact that they have a different chemical composition. Increasing the concentration of ALG and MUC in the dispersions resulted in an increase of the shear viscosity. León-Martínez et al. [25] found that *Opuntia ficus-indica* mucilage forms viscous aqueous dispersions, exhibiting a shear-thinning behavior and shows important viscoelastic properties. They observed a predominantly elastic behavior $G' > G''$, known as solid-like behavior, for a dispersion of lyophilized mucilage powder at concentrations >3% (w/v) and times >0.2 s. Mucilage's rheological properties are mainly a function of its concentration, pH, ionic strength, frequency and temperature [26].

Table 6
Rheological model parameters for aqueous dispersions at different concentration levels and 25 °C.

Sample's name – concentration (w/v)	Ostwald-de Waele model parameters $\eta(\dot{\gamma}) = k\dot{\gamma}^{n-1}$		
	$k \times 10^{-2}$ (Pa s^n)	n (–)	R^2 (–)
MUCD – 8.7 g L^{-1}	1.0817	0.7614	0.999
MUCD – 7.2 g L^{-1}	0.9671	0.7514	0.979
MUCD – 3.6 g L^{-1}	0.5799	0.7353	0.905

Sample's name – concentration (w/v)	Sisko model parameters $\eta(\dot{\gamma}) = k\dot{\gamma}^{n-1} + \eta_\infty$			
	$\eta_\infty \times 10^{-3}$ (Pa s)	$k \times 10^{-2}$ (Pa s^n)	n (–)	R^2 (–)
ALGD – 20 g L^{-1}	5.9168	3.0361	0.1387	0.999
ALGD – 10 g L^{-1}	2.3150	1.2795	0.0100	0.979
ALGD – 5 g L^{-1}	1.7115	0.3439	0.1291	0.905

Sample's name – concentration (w/v)	Cross model parameters $\frac{\eta(\dot{\gamma})-\eta_\infty}{\eta_0-\eta_\infty} = \frac{1}{1+(K\dot{\gamma})^m}$				
	η_0 (Pa s)	$\eta_\infty \times 10^{-8}$ (Pa s)	$K \times 10^{-2}$ (s)	m (–)	R^2 (–)
Na-AlginateD – 20 g L^{-1}	5.0663	2.4776	35.4020	0.6328	0.969
Na-AlginateD – 10 g L^{-1}	0.3719	1.4000	3.6543	0.7320	0.998
Na-AlginateD – 5 g L^{-1}	0.0696	0.3052	6.0659	0.5103	0.907

–For further information about each parameter in the flow models see Mezger [18] and Barnes [24].

The rheological behavior of Na-alginate dispersions exhibits both a Newtonian region and a shear-thinning region. The first region is observed as a plateau where the viscosity remained constant with increasing shear rate, up to a certain value of shear rate. Therefore, in this dispersion the zero-shear viscosity (Eq. (1)) was very important and the best fit to the experimental data was obtained with the Cross model. This behavior could be explained by the entanglements of the chains of polysaccharide at low shear rates (see [18,24]. Viscosity increases significantly with increasing degree of entanglement (η_0).

$$\eta_0 = \lim_{\gamma \to 0} \eta(\dot{\gamma}) \tag{1}$$

The dependence of the shear-viscosity with respect to the concentration was more pronounced in Na-alginateD compared to MUCD and ALGD, being more evident at low shear rates. Smith and Miri [27] have mentioned that in concentrated alginate dispersions the viscosity is highly dependent upon the molecular mass. The viscosity increases with increasing molecular mass. Other factors such as Guluronic acid to Mannuronic acid ratio, pH, ionic strength and, in particular, the presence of divalent cations, can cause variations in the viscosity.

The viscosity curves of Na-alginateD were higher than those measured in ALGD at the same concentrations. To explain this, we must consider the following. In untreated algae, the alginates represent 10–40% of its dry weight. Therefore, other chemical compounds with different molecular weight and structure such as other polysaccharides (xylans, mannans and fucoidan), proteins, amino acids, lipids, minerals and saccharides of low molecular weight [28], do not contribute to the viscosity in same way as pure alginates. In addition, the polydispersity of the alginate's chains is another factor contributing to the viscosity.

3.3. Flow behavior of cement pastes and mortars subjected to steady-shear

Characterization of deformability and viscosity of SCC in fresh state is critical and it is usually performed through tests such as slump-flow or V-funnel [5]. An appropriate combination of rheological parameters such as yield-stress, viscosity and thixotropy

[29,30] are required to obtain a fresh concrete with high fluidity and resistance to segregation. Generally, these parameters are evaluated by fitting flow curve data to rheological models such as Bingham and Herschel–Bulkley. SCC sometimes is best represented by the Herschel–Bulkley model, since negative values of yield-stress can appear using the Bingham model [31,32].

Fig. 5 presents the viscosity curves of the cement pastes studied. It is observed that all the cement pastes exhibited a non-linear behavior, which is represented to some extent by the Herschel–Bulkley model (Eq. (2)).

$$\tau = \tau_0 + k\dot{\gamma}^n, \quad \tau \geqslant \tau_0 \tag{2}$$

where τ_0 is the Herschel–Bulkley yield-stress (Pa), k is a consistency index (Pa s^n), n is a dimensionless flow behavior index, $\dot{\gamma}$ is the shear rate (s^{-1}), and τ is the shear stress (Pa).

Yield-stress is the shear stress required by a 'viscoplastic' material to flow like a viscous liquid and it occurs when the shear stress becomes independent of the shear strain and the system behaves as a solid, that is, it will not flow [23].

Results of the fitting analysis are presented in Table 7. In general, τ_0 increases with increasing VEA concentration. Therefore, workability of concrete is adversely affected. Notice that the flow behavior of the cement paste with ALG-0.5% is similar to CP_0. This means that the inclusion of ALG increases both τ_0 and $\eta(\dot{\gamma})$. The effect of SP is negligible and the yield-stress is 52 times greater than in cement paste containing the commercial VEA (RP). In SCC the SP is incorporated to decrease τ_0.

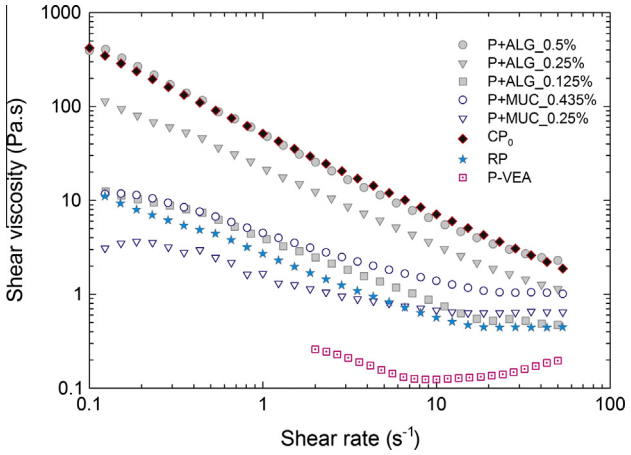

Fig. 5. Flow curves of cement pastes at 25 ± 0.2 °C with different types and concentrations (%w) of VEAs.

In almost all cases the flow index was <1. This indicates a shear-thinning behavior, except for the cement paste with ALG-1%, for which a shear-thickening behavior was observed. That is, there is an increase of shear viscosity with increasing shear rate or shear stress.

The inclusion of MUC in both cement pastes and mortars produced a more pronounced shear-thinning behavior than ALG at the same concentrations. This difference may be attributed to the polymer characteristics such as structure, architecture, polydispersity, chain length, molecular mass and molecular conformation in the dispersion. A common explanation of shear-thinning behavior is that the input shear energy tends to align anisotropic molecules or particles, and tends to disaggregate large clusters of particles; thereby reducing the overall hydrodynamic drag. This reduction in turn reduces both the dissipation of energy in the fluid and the viscosity [24].

It is known that cement paste generally shows shear-thinning behavior because the cement particles tend to form flocs. If the shear rate is increased, these flocs are broken in primary particles accompanied by a reduced resistance to flow, therefore the viscosity is reduced. This behavior can be observed in the control samples, where flocculation takes place. But the viscosity of cement pastes may also depend on time. During loading–unloading cycles in steady-shear experiments, the cement paste presents a certain area of hysteresis due to the change of slope in their ascending-descending flow curves. This hysteresis area represents a quantitative measurement of the energy necessary to disturb the structure of a given volume of paste following some period of rest and it is an indicative of thixotropic properties [30]. However, the thixotropic effects produced by the flocculation process and the formation of CSH bridges between cement particles can be neglected in almost all the tested samples, where the SP dosage was used at the saturation point. At this point the SP has been adsorbed completely on the cement particle surface, therefore the cement particles are dispersed and the flocculation process is delayed, allowing time for the rheological tests. The addition of SP causes an increase in the fluidity of the paste and changes its behavior from shear-thinning to Newtonian. However, in some instances it can result in shear thickening. This happened on the cement paste without any VEA, where the SP causes a significant reduction in the τ_0 value in

Table 7
Calculated rheological properties of cement pastes and mortars at different VEA concentrations and 25 °C.

	Viscoelastic properties					Flow properties Herschel–Bulkley parameters			
Sample	VEA %w	τ_y Pa	τ_f Pa	γ_L %	Crossover modulus Pa	τ_0 Pa	k Pa s^n	n –	R^2 –
P + ALG	0.125	0.152	1.433	0.037	4.312	1.655	1.891	0.569	0.957
	0.250	1.150	8.795	0.058	15.210	0.089	21.519	0.210	0.968
	0.500	3.672	21.560	0.082	26.170	49.085	0.799	1.119	0.992
P + MUC	0.250	0.270	0.675	0.061	11.330	0.015	1.547	0.676	0.919
	0.435	0.420	1.518	0.098	12.980	0.372	3.982	0.565	0.954
CP_0	0	3.167	10.914	0.036	40.708	40.877	9.884	0.455	0.999
RP	0.065	0.008	0.439	0.025	6.600	0.934	1.923	0.600	0.952
P-VEA[a]	0	–	–	–	–	0.490	0.019	1.575	0.999
M + ALG	0.125	1.200	8.697	0.031	29.040	10.000	43.021	0.492	0.926
	0.250	6.090	20.900	0.037	63.940	39.591	32.591	0.580	0.983
	0.500	15.040	78.340	0.047	111.700	155.130	0.707	1.455	0.882
M + MUC	0.250	1.660	9.350	0.015	64.410	0.500	38.534	0.598	0.791
	0.435	14.000	43.925	0.046	40.740	9.000	139.120	0.268	0.945
CM_0	0	28.340	97.060	0.047	68.930	134.180	3.690	0.974	0.953
RM	0.065	0.939	10.020	0.031	32.770	12.282	39.629	0.491	0.963

[a] The dynamic test was not made on this sample.

comparison with the control paste (see Table 6). Jayasree et al. [33] found that the hysteresis area in loading–unloading experiments in steady shear decreases with increasing SP dosage, obtaining the maximum reduction approximately at the saturation dosage of the SP. Therefore, in our study the observed thixotropic effect is related to the inclusion of the proposed VEAs, depending on the type of bonds and/or physical interactions between molecules that take place especially at low shear rates.

The shear-thickening behavior of SCC could be explained by two possible theories [31,34]. The first theory refers to the formation of clusters, which are temporary assemblies of small particles formed at certain shear stress, therefore increasing viscosity with increasing shear stress. The second one is based on grain inertia, where a part of the shearing force is transmitted through direct momentum transfer between solid particles [31]. According to Roussel et al. [34] the van der Waals forces dominate the hydrodynamic forces at low strain rate regime and give raise to a macroscopic shear-thinning behavior. At intermediate strain rates the hydrodynamic forces dominate, and finally the particle inertia dominates the high strain rates response and may lead to shear-thickening.

To determine which of these two theories may better explain the observed behavior in the cement pastes and mortars, the ratio of inertial to viscous forces were calculated according to Feys et al. [31]. The particle Reynolds number was calculated considering the maximum shear rate of 50 s^{-1} used in the experiments. For cement paste, a density of 2380 kg m^{-3}, a maximum cement particle radius of 150 μm and a viscosity of 2.5 Pa s (at a shear rate of 50 s^{-1}) were considered. For mortar a density of 2516 kg m^{-3}, a maximum sand particle radius of 600 μm, which corresponds to the 92.5% of the sample and a viscosity of 7 Pa s (at shear rate of 50 s^{-1}) were considered. The results indicated values of particle Reynolds number of $1 \times 10^{-3}$and 6.4×10^{-3} in pastes and mortars, respectively. As these values are <0.1, then the grain inertia can be neglected and shear-thickening was probably caused by cluster formation [31]. In the case of mortar containing ALG-0.5%, the inclusion of silica sand increased the volume fraction of solid particles from 0.392 to 0.697 compared to a cement paste. This in turn increased the intensity of the shear-thickening in the mortar (see the flow coefficient n in Table 7).

At low shear rates (<1 s^{-1}) MUC provides less viscosity to cement pastes compared to ALG (see Fig. 5). This may be explained by the difference between structure and molecular mass of both proposed VEAs. For example, entanglements between mucilage chains were not observed in MUC aqueous dispersions at the concentrations used. However, the MUC exhibited a better flow behavior in the full range of shear rates studied. With MUC, τ_0 was not significantly increased and the shear viscosity was higher at high shear rates in comparison with RP. This ensures a higher stability of the cement paste at high shear rates and a higher flowability at low shear rates in comparison with ALG paste. The increase in shear viscosity can be attributed to the fact that the degree of water retention by the polymer increases with increasing VEA concentration [10].

In addition, it was observed that samples containing ALG incorporated air bubbles that were stable for a long time. The proteins in ALG act like a surfactant that stabilizes air bubbles in the suspensions. A high viscosity prevents the bubbles from rupturing or coalescing by creating a 'cushion effect', therefore they are unaffected by mixing and other disturbances. Inclusion of air produced important effects on the rheological behavior of the fresh samples. This characteristic could be a disadvantage for the compressive strength of SCC, unless this VMA is partly replacing air-entraining agents for SCC exposed to freeze–thaw conditions, provided it ensures and adequate air system. Łaźniewska-Piekarczyk [7] reported that small dosages of air-entraining admixture may result in an increase of the flow diameter. However, higher dosages of air entraining admixture in SCC decreases the flow diameter due to higher interaction between the air bubbles and the cement particles and aggregates.

Fig. 6 presents the viscosity curves for mortars. There is a significant increase on the viscosity due to the sand inclusion. It is observed a remarkable performance of MUC at high shear rates. This could be explained by the adsorption of part of the water on the sand grains' surface. Therefore, the available water for lubricating effect is retained within the polymer chains, making the mixture more viscous.

MUC chains can establish certain physical bonds with the adsorbed water by hydrogen bonds and shear-thinning behavior is observed. The non-linear fitting was affected by the values of shear stress at low shear rate in the mortar containing ALG-0.5%, which presented a value of $n = 1.45$ (Table 7) and a value of τ_0 closer to the one obtained in the CM_0, being its determination coefficient <0.95. The viscosity curve of mortar containing ALG-0.125% was similar to the RM and the smallest value of the τ_0 corresponds to the mortar containing MUC-0.25%.

Lachemi et al. [10] reported that plastic viscosity of Portland cement mortar increased, while the yield-stress decreased with an increasing concentration of VEA based in polysaccharides at a fixed dosage of SP. However, they used the Bingham model to fit the experimental flow data.

In our study we observed an increase in τ_0 values with increasing concentration of ALG, except in the case of cement paste with ALG-0.25% (see Table 7). Sometimes, the calculated coefficient R^2 was smaller than 0.95 when fitting the experimental data to the Herschel–Bulkley model. This indicates the difficulty of measuring the 'real yield-stress', as the lowest shear rate used in the steady-state test was 0.1 s^{-1}, which is limited mainly by the geometry used. The 'real yield-stress' implies an elastic solid (Hookean) behavior in the limit when the shear rate approaches zero, as in the Bingham viscoplastic model [24]. In some cases, obtaining an essentially horizontal region in a double-logarithmic plot of shear stress against strain rate is considered the most satisfactory criterion for the existence of a yield-stress.

For this study, the Herschel–Bulkley yield-stress was increased with increasing concentration of any VEA, being more marked with ALG than with MUC. Khayat [9] reported that the incorporation of VEA in cement-based materials increases the yield-stress, the plastic viscosity and the apparent viscosity, at both low and high shear rates, regardless of the water to cement ratio and SP dosage. Leemann and Winnefeld [35] have also reported that at fixed water to binder ratio, the addition of VEA causes a decrease of mortar

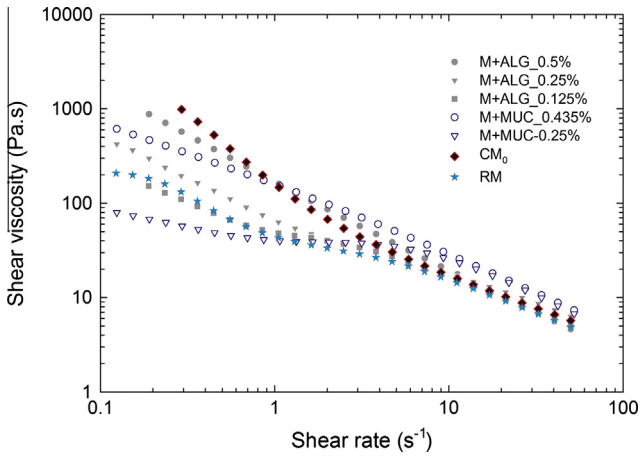

Fig. 6. Flow curves of mortars at 25 ± 0.2 °C with different types and concentrations (%w) of VEAs.

flow and an increase in flow time (V-funnel test), which corresponds to an increase in both the yield-stress and the plastic viscosity, respectively.

3.4. Strain amplitude dependence of the cement pastes and mortars

Typical plots of amplitude sweep tests are shown in Fig. 7, where only the results obtained for some cement pastes are presented. Fig. 7-A shows the storage (G') and the loss (G'') modulus against the strain amplitude. It permits identification of the LVE region, where the structural characteristics of a sample are known [18]. In this region, the shear stress is proportional to the shear strain and the rheological parameters (G' and G'') are expected to be independent of the applied stress or strain. In order to establish the LVE region, the rheological parameters are measured as a function of strain amplitude, while the frequency is kept constant. The position and length of the LVE indicate the property of the sample to resist flow and maintain its stability over a range of stresses. The γ_L is the limiting value of strain amplitude. Below this value, the dynamic modulus reaches a plateau value. At amplitudes higher than γ_L, where the dynamic modulus decreases, the structure of the sample is irreversibly changed or even completely destroyed [18].

Each of the cement pastes containing ALG and MUC dispersions had a similar behavior to the one containing ALG-0.5% (see Fig. 6-A), where $G' > G''$ at low strains, showing a solid-like behavior. Cement pastes and mortars containing ALG or MUC exhibited a better micro-structuration than reference samples (RP or RM), indicated by higher values of γ_L. As a consequence the stability increases with increasing critical strain amplitude. This stability combined with a small flow stress is essential for SCC.

A summary of the analysis of cement pastes and mortars is presented in Table 7. In the cement pastes γ_L ranged from 0.025–0.098%, while in the mortars it ranged from 0.015–0.047%. The LVE region increased with increasing concentration of ALG or MUC, being more noticeable in cement pastes than in mortars. In the mortars, the LVE region was reduced as a result of the inclusion of sand particles, which prevent direct contact between polymer–polymer (entanglements) and between cement particles. The contact points between cement particles are created by the early hydrates [36]. Therefore, the structure of the material is weakened and the network structure is disrupted at shorter strain amplitudes.

Fig. 7-B shows a typical response of G' and G'' against shear stress for the cement pastes containing ALG at two different concentrations. The 'yield-stress' (τ_y) and 'flow stress' (τ_f) were determined by plotting the response for each of the mortars and cement pastes tested. τ_y corresponds to the limiting value of the LVE region in terms of the shear stress. No significant changes of the internal microstructure occur as long as the stresses below the yield point are applied. τ_f corresponds to the crossover point where $G' = G''$, the solid viscoelastic behavior with $G' > G''$ changes to a liquid behavior with $G'' > G''$ [18].

It is important to mention that the yield-stress obtained in oscillatory tests is several times less than the one obtained in steady shear tests, in which a flow model is used to determine the yield-stress (e.g. Bingham model). This is because sometimes the independence of the shear stress with the shear strain is not reached in the steady-shear test. The asymptotic non-zero value of the shear stress is not found with the minimum shear rate used in the experiments, and then the value estimated of yield-stress is an 'apparent value'. Oscillatory tests are considered non-destructive. In this case, τ_y represents the critical value of shear stress, the point at which the elastic modulus has lost its constant behavior with respect to shear stress 'yield point'. This value represents small changes in the particle–particle contacts [34,36] and at shear stresses higher than τ_y, a non-linear behavior starts. In addition, some problems observed by Schatzmann et al. [19] for the BMS are the tool acceleration, wake formation and viscous over stream, sphere interaction with suspended particles, effect of pre-structured samples, data scattering due to grain size, temporary jamming, and side effects (distance between the sphere and the container boundary). All of these may affect the estimation of the real shear stresses in steady-shear tests.

It was observed that both yield-stress and flow stress increased dramatically with increasing concentration of VEAs. In the case of ALG, the increase followed a power–law relationship, as indicated by the following equations:

$$\tau_f = A|C_{ALG}|^{1.77}, \quad R^2 = 0.962 \tag{3}$$

$$\tau_y = B|C_{ALG}|^{20.6}. \quad R^2 = 0.947 \tag{4}$$

where, C_{ALG} is the concentration of aqueous dispersion of ALG, A and B are fitting parameters that depend on the type of cement-based material (cement paste or mortar).

If the concentration of ALG in the mixing water is 0.5% in cement pastes or mortars, then the values of τ_y and τ_f are close to the values of the CP_0 and CM_0, respectively, despite of the presence of SP. A similar behavior was observed in the steady shear tests. It may be that the entanglements between macromolecules of VEA maintain the internal structure and increase the LVE range. For all of the samples, τ_f value was always higher than τ_y, which indicates that τ_f is more important than τ_y in terms of mixing

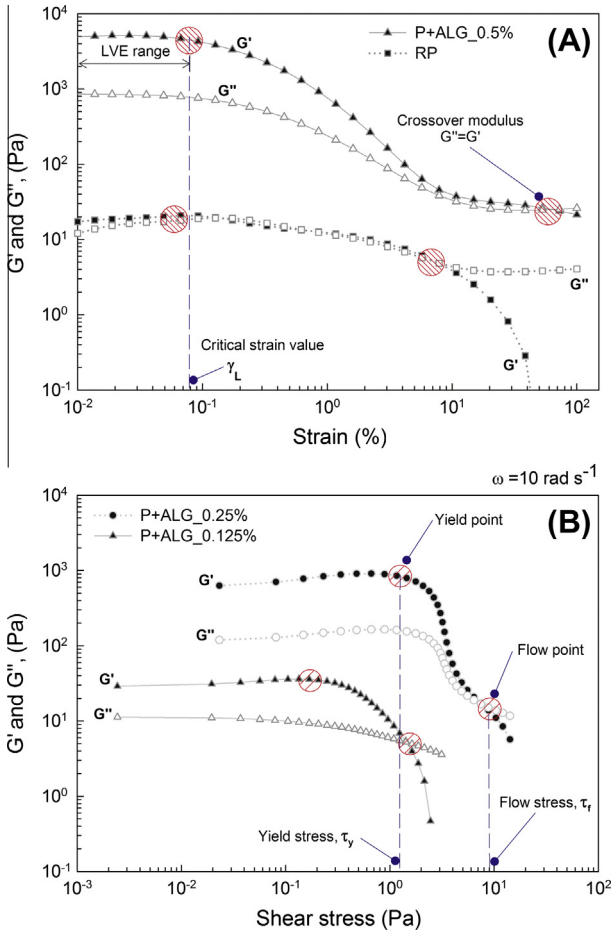

Fig. 7. Typical plots of amplitude sweep test results. (A) Storage modulus G' and loss modulus G'' against strain amplitude. (B) G' and G'' against shear stress.

energy. The 'flow stress' is comparable to the Herschel–Bulkley yield-stress, and represents the energy necessary to break down the interaction between particles to allow the system to flow. Roussel et al. [34] have identified four main types of interactions: colloidal forces, Brownian forces, hydrodynamic forces and contact forces between particles. Depending on the size of the particles, their volume fraction in the mixture and on external forces, one or several of these interactions dominate.

Fig. 8 is a schematic representation of the possible behavior of ALG in cement paste. The SP molecules are adsorbed on the surface of cement particles, producing their dispersion mainly by steric hindrance [7]. However, a part of the water molecules are enclosed in the network formed by the polymer chains. Therefore, they do not contribute to the flowability of the paste. At low shear strain, the ALG chains can form entanglements between themselves and possibly with the SP chains, which generates a transient network that should disappear when the strain rate or shear stress increase. This is observed as a shear-thinning behavior. Sonebi et al. [37] observed similar trends when they studied diutan and welan gum. In addition, some divalent cations (Ca^{2+}, Mn^{2+}, Mg^{2+}) available at the surface of cement particles and in dispersion could form intermolecular junction zones with the carboxylate groups on the guluronate residues of adjacent polymer chains, resulting in a weak gel structure formation [27].

On the other hand, the rheological behavior of MUC indicates another mechanism responsible for increasing the viscosity of cement-based materials, since the entanglements were not observed in the cement pastes and mortars with 0.435%. Some authors [25,26,38] suggest a random coil conformation for this polymer. Probably, the overall shape of the MUC chain is more spherical than the ALG, resulting in shrunken polymer chains. In consequence, the viscosity is lower at low strain rate at the same concentrations, but the MUC is able to retain more water at higher strain rates. The rheological properties of MUC depend to a higher degree on the molecular conformation of mucilage in dispersion [26]. The higher molecular mass of MUC could explain its higher water retention. For MUC it ranged from 2.3 $\times 10^4$ to 3 $\times 10^6$ g mol^{-1} [26,38] and for ALG it may range from 5 $\times 10^4$ to 6 $\times 10^5$ g mol^{-1} [39]. The hydroxyl groups along the MUC chains can bond to water molecules through hydrogen bonds, so their apparent volume increases by swelling, which in turn increases the viscosity of the mixing solution [40]. When the strain rate increases, a part of water is released and the shear-thinning phenomenon is observed. Sonebi et al. [37] observed a higher viscosity in diutan gum, which has a higher molecular mass than welan gum. Knowledge of polysaccharide molecular shape and its effects on the intermolecular interactions are essential to understand and control the rheological properties of SCC.

Viscoelasticity and shear-thinning behavior indicate thixotropic properties of fluids, which increase the stability of concrete and reduce the risk of segregation after casting [7].

Viscoelastic substances such as fresh cement-based materials react with a temporal delay, which is expressed by a phase shift angle δ. Since $0 \leqslant \delta \geqslant \pi/2$ phase angles of 0 rad and $\pi/2$ rad indicate purely elastic and viscous materials, respectively. When $G' = G''$, the value of phase angle is $\pi/4$ rad, the modulus value at this point is called the crossover modulus and the material is changing from a solid like to a liquid behavior or vice versa [18,24].

Figs. 9 and 10 show the δ as a function of the strain amplitude for cement pastes and mortars, respectively. The RP maintained a $\delta > 0.7$ rad, indicating weak gel characteristics at strain amplitudes <5%, approximately. Beyond this value, the damping factor was $>\pi/4$ rad, indicating a more liquid behavior. In spite of having a

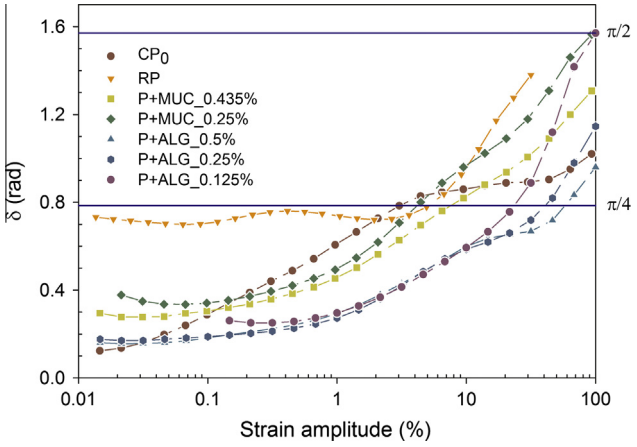

Fig. 9. Phase angle (δ) as a function of the strain amplitude (γ) for cement pastes containing VEAs. The angular frequency (ω) was 10 rad s^{-1} at 25 ± 0.2 °C.

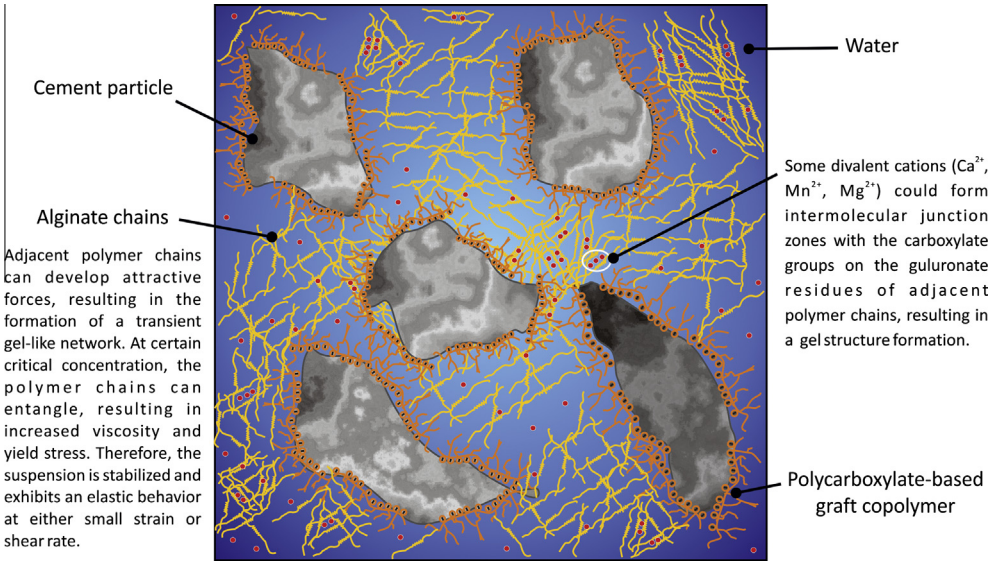

Fig. 8. Schematic representation of the network formation between the ALG polymer chains in cement pastes.

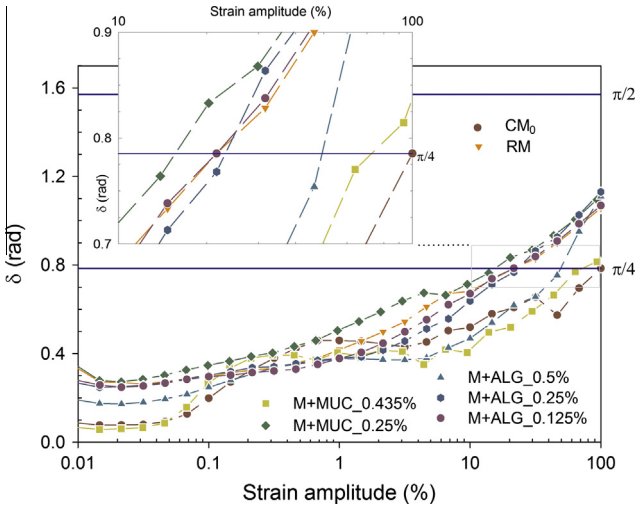

Fig. 10. Phase angle (δ) as a function of the strain amplitude (γ) for mortars containing VEAs. The angular frequency (ω) was 10 rad s^{-1} at 25 ± 0.2 °C.

lower concentration of the commercial VEA compared to that of MUC or ALG, its effect on τ_y was less important. The main component of the commercial VEA is welan gum, which has a molecular mass ranging from 6.6 $\times 10^5$ to 9.7 $\times 10^5$ g mol^{-1}. It is composed of tetra-saccharide repeating units of D-glucose, D-glucoronic acid, D-glucose, and L-rhamnose, with L-rhamnopyranosyl or L-mannopyranosyl side chains [37]. Long chain molecules can adhere to the periphery of water molecules, adsorbing and fixing part of the mixing water and increasing the yield point and plastic viscosity.

Cement pastes containing MUC and ALG presented lower values of δ than RP at strain amplitude <1%, which indicates highly structured materials where short-range interactions are very important. In this case, the interactions between the VEAs' chains might generate and increase the strength of the microstructure. The CP_0 was the most rigid material at strain amplitudes <0.02% (see Fig. 9), suggesting that the particles are held together due to attractive interactions via colloidal forces [34].

The cement paste with MUC-0.25% presents the crossover modulus at shorter strain amplitude than ALG at the same concentration, even when compared with the RP. The equilibrium between elastic and viscous behavior was reached at short strain amplitudes when MUC is added to the mixture. The magnitude of the crossover modulus for cement pastes and mortars with both proposed VEAs was always higher than the reference samples, conferring to the mixture a more elastic behavior (see Table 7).

An increase in the plasticity of mortars with MUC has been reported by Chandra et al. [16]. According to Cárdenas et al. [11] the cactus extract produced a reduction of the maximum stress and deformation values of pastes with calcium hydroxide and slaked-lime compared to their control samples. They found that at low cactus extract concentrations, the mucilage reduced the continuity of the network. As the concentration was increased, the mechanical properties also increased due to the formation of a more homogeneous network. This could be explained by the reduction in the contact points between solid particles by adsorption of mucilage on their surface. This is in agreement with the flow and dynamic behavior observed in this study for the paste and mortar with MUC-0.25%, where τ_0 and τ_f were slightly lower than in the reference sample, probably caused by steric hindrance of the polymer chains between particles and by its shear-thinning behavior. However, some bleeding was observed in cement pastes and mortars at longer times, indicating viscosity dependence of MUC on the pH and on the presence free cations. This indicates that MUC may be needed at a higher concentration.

In the case of mortar with ALG-0.125% and RM, it is observed a similar behavior and the elastic properties dominate over viscous properties at strain amplitudes <10% (Fig. 10). Mortar with MUC showed better viscous characteristics at intermediate strain amplitude (0.1–10%). CM_0 showed the strongest solid-like behavior. For all the mixtures (pastes and mortars) with ALG the values of δ were lower with an increasing concentration. This reflects the greatest influence of ALG on flow and elastic properties of cement-based systems.

3.5. Preliminary SCC incorporating the proposed new VEAs (MUC and ALG)

From the results obtained in the cement pastes and mortars, it was decided to use the proposed VEAs at two levels of concentration 0.25% and 0.50%, both with a SP dosage of 0.321% with respect the cement weight (see Table 5). However, it was not possible to obtain MUC at 0.50%. Therefore, it was used at 0.374% with a lower dosage of SP (0.257%). A replicate of ALG-0.25% with a lower dosage of SP (0.276%) was also made.

Table 8 provides the properties measured on the preliminary SCC mixtures. The slump flow varied between 430 mm and 800 mm. Although the concrete with MUC-0.25% had the highest value of flow spread, it was observed high degree of bleeding, which could be explained by the low viscosity of the cement paste.

The reference concrete exhibited high stability and high flow spread, followed by the concrete with ALG-0.25% (Fig. 10).

Using flow spread data and the Murata and Roussel approaches reported by Flatt et al. [41], the concrete yield-stress was calculated (Table 8). However, the values obtained with the Roussel approach were omitted because they were much lower than the experimental values obtained in the mortars. In order to compare the concrete yield-stress obtained with the Murata equation, based on the spread radius, to the experimental yield-stress from mortars, the empirical equation obtained by Goaszewski [42] was used. This equation allows calculating the yield-stress of a concrete based on the relative volume of mortar in the concrete (0.709 for our concrete) and the yield-stress of the mortar (data from Table 7). The results are presented in parentheses in Table 8. The magnitudes of both yield-stresses were similar, except for the SCC1. Also, it was observed that small changes in the yield-stress of mortar may be accompanied by substantial changes in the yield-stress of fresh concrete, whence on its flowability.

The mixtures containing ALG always exhibited a higher yield-stress than the MUC at the same concentration. Some concretes containing ALG and MUC were stable and homogeneous mixtures, where the optimal concentration depends on the polymeric nature and the polymeric interaction with the cement particles. The static segregation percent was >4.5% only in the case where the VEA concentration was 0.25% with 0.321% of SP. This was probably due to the thixotropy of concrete, where the recovery time (time for build-up structure in the cement paste) was not short enough. Therefore, the static yield-stress would no rapidly increase to improve the segregation resistance. The thixotropic effect of the inclusion of these proposed new VEAs should be studied in the future.

In general, SCC with ALG exhibited high stability and cohesiveness during the slump flow test (Fig. 11). Trapped air bubbles in the concrete play a role in this stability. The surfactant effect of proteins contained in ALG produced this high levels of air in the mixture >6%. This concrete could resist freeze–thaw cycles, provided it has an adequate air system. These results are promising and more formulations of SCC with ALG and MUC should be done to study

Table 8
Fresh properties of SCC mixtures containing different types of VEAs.

Test	Measurement	RSCC Welan gum-0.065%	SCC1 MUC-0.250%	SCC2 MUC-0.374%	SCC3 ALG-0.250%	SCC4 ALG-0.250%	SCC5 ALG-0.500%
Slump flow	Flow spread (mm)	753	800	701	736	705	430
	$T_{50\ cm}$ time (s)	1.3	1.2	1.2	1.5	0.3	[c]
	VSI (0–3)	0	3	1	2	0	0
	Yield-stress (Pa)[a]	191.65 (179.45)	169.56 (167.45)	223.62	201.10 (374.30)	211.64	561.17 (1403.01)
J-Ring with inverted slump cone	J-ring flow spread (mm)	723	730	645	625	640	395
	Height difference (mm)	0.48	1.30	0.50	1.50	0.83	1.40
V-Funnel	T-0 (s)	4.32	3.43	5.10	6.74	3.42	5.52
	T-5 (s)	4.52	29.00	5.11	6.81	3.48	5.68
	Average flow-through speed, V_m ($m\ s^{-1}$)[b]	0.475	0.598	0.402	0.304	0.600	0.372
	Flow-through index, S_f (–)[b]	0.046	7.454	0.002	0.01	0.017	0.029
L-Box	Blocking ratio h_2/h_1 (–)	0.94	0.51	0.67	0.46	0.93	0.51
Segregation column	Percentage of static segregation (%)	0.28	7.70	0.48	4.54	3.28	2.36
Other properties	Air content (v%)	0.80	0.60	1.25	2.57	6.00	6.20
	Unit weight ($kg\ m^{-3}$)	2280	2280	2310	2290	2210	2180
	Temperature (°C)	17	21	18	21	20	19
Observations		A highly stable mixture was observed	Excessive bleeding was observed together with visible segregation	A slight aggregate pile in the center of the concrete mass was observed	A stable and homogeneous mixture with a slight halo of bleeding was observed	A stable and homogeneous mixture was observed	A stable and homogeneous mixture was observed

[a] Data calculated using the Murata equation with 3D yield criteria given in Flat et al. [41] and the data between parentheses were calculated using the empirical equation from Goaszewski [42], where a value of relative volume of mortar in the concrete of 0.709 was used in the computations.
[b] These were calculated using the Eqs. (3)–(13) and (3)–(14) reported in [23].
[c] There was not any flow due to very high yield-stress of the mixture.

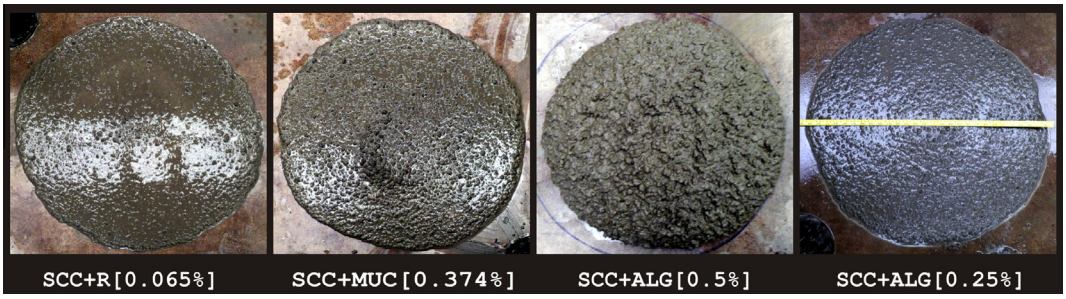

Fig. 11. Visual appearance of SCC mixtures containing MUC, ALG and a commercial VEA during the flow spread test at room temperature.

their rheological properties in fresh state as well as their mechanical and durability properties in hardened state.

4. Conclusions

This paper has focused on the study of two new viscosity-enhancing admixtures: nopal mucilage and marine brown algae extract in cement based materials. In the first part, the viscosity curves of the VEAs dispersions were determined, and the rheological properties of cement pastes and mortars were studied under both rotational and oscillatory shear tests. In the second part, trial SCC mixtures were made incorporating the admixtures and their fresh properties were compared with an SCC containing a commercial VEA.

The main conclusions are as follow:

- Aqueous dispersions of nopal mucilage (MUC) and brown algae extract (ALG) exhibited a shear-thinning behavior ($n < 1$), being the algae extract more viscous than nopal mucilage at low shear rate (<1 s^{-1}).
- In steady-shear tests on cement pastes and mortars, increasing the concentration of the proposed VEAs produces an increase in Herschel–Bulkley yield-stress and shear viscosity. The brown algae extract had the highest effect on Herschel–Bulkley yield-stress.
- Strain amplitude sweep tests made on cement pastes and mortars showed that the flow stress in oscillatory test is more related to the Herschel–Bulkley yield-stress. The flow and yield stresses followed a power–law relationship with respect to ALG concentration, having a power around 1.77 and 2.06, respectively.
- ALG increases the air content in the mixture due to its protein content, being in some cases >6%.
- MUC increases and maintains a higher viscosity at shear rates >5 s^{-1}, without significantly increasing on yield-stress in comparison with ALG. Therefore provides a better rheological behavior of mortars.
- ALG and MUC present a solid-like behavior at short strains (<1%), being more evident in mixtures containing ALG due to the interaction between polysaccharide chains that creates a gel network, thus producing a stiffer microstructure.
- Use of the BMS in oscillatory shear mode to characterize suspensions containing large particles allows one to obtain the yield-stress in the limiting value of LVE, the flow-stress, the phase angle ($\delta < \pi/2$) and other important viscoelastic parameters.
- Some preliminary SCC mixtures containing MUC or ALG at concentrations >0.25% were stable and homogeneous with slump flow values higher than 700 mm, indicating that both ALG and MUC exhibit adequate characteristics to be used as VEAs.

Future work

In order to establish a better understanding of the rheological behavior of nopal mucilage and optimize the rheology of fresh cement-based materials, it is necessary to determine its behavior under alkaline media, in order to mimic the process happening after the cement is in contact with water. It is also necessary to study its rheological behavior in the presence of different cations. Another important aspect is to confirm the presence of protein fraction in the nopal mucilage.

Acknowledgments

The authors would like to thank Instituto Politécnico Nacional from Mexico for funding the project with ID code SIP-20120415. They also thank the Consejo Nacional de Ciencia y Tecnología (CONACyT) and the company "Herrozinc S.A. de C.V." for funding the project with ID code 137669. We would like to thank Professor G. Haley for the revising of English language in this manuscript. Finally, we would like to thank to the anonymous reviewers by their important contributions made to improve this paper.

References

[1] Schneider M, Romer M, Tschudin M, Bolio H. Sustainable cement production-present and future. Cem Concr Res 2011;41(7):642–50. http://dx.doi.org/10.1016/j.cemconres.2011.03.019.
[2] Plank J. Applications of biopolymers and other biotechnological products in building materials. Appl Microbiol Biotechnol 2004;66(1):1–9. http://dx.doi.org/10.1007/s00253-004-1714-3.
[3] Dransfield J. Admixtures for concrete, mortar and grout. In: Newman J, Choo BS, editors. Advanced concrete technology, constituent materials. Oxford: Butterworth-Heinemann; 2003.
[4] Nanthagopalan P, Santhanam M. A new empirical test method for the optimization of viscosity modifying agent dosage in self-compacting concrete. Mater Struct 2010;43:203–12. http://dx.doi.org/10.1617/s11527-009-9481-3.
[5] Okamura H, Ouchi M. Self-compacting concrete. J Adv Concr Technol 2003;1(1):5–15.
[6] Gaimster R, Dixon N. Self-compacting concrete. In: Newman J, Choo BS, editors. Advanced concrete technology, processes. Oxford: Butterworth-Heinemann; 2003.
[7] Łaźniewska-Piekarczyk B. The influence of selected new generation admixtures on the workability, air-voids parameters and frost-resistance of self-compacting concrete. Constr Build Mater 2012;31:310–9. http://dx.doi.org/10.1016/j.conbuildmat.2011.12.107.
[8] Collepardi M. Admixtures used to enhance placing characteristics of concrete. Cem Concr Compos 1998;20(2–3):103–12. http://dx.doi.org/10.1016/S0958-9465(98)00071-7.
[9] Khayat KH. Viscosity-enhancing admixtures for cement-based materials – an overview. Cem Concr Compos 1998;20(2–3):171–88. http://dx.doi.org/10.1016/S0958-9465(98)80006-1.
[10] Lachemi M, Hossain KMA, Lambros V, Nkinamubanzi P-C, Bouzoubaâ N. Self-consolidating concrete incorporating new viscosity modifying admixtures. Cem Concr Res 2004;34(6):917–26. http://dx.doi.org/10.1016/j.cemconres.2003.10.024.
[11] Cárdenas A, Arguelles WM, Goycoolea FM. On the possible role of *Opuntia-ficus-indica* mucilage in lime mortar performance in the protection of historical buildings, Journal of the Professional Association for Cactus Development

1998;3:64-71. <http://www.jpacd.org/downloads/Vol3/RAC_4.pdf>, [accessed 4.09.2012].
[12] Torres-Acosta AA, Cano-Barrita PF de J. Las bondades del nopal. Construcción y Tecnología 2007;233:44-49. <http://www.imcyc.com/ct2007/oct07/tecnologia.htm>, [accessed 4.09.2012.
[13] Torres-Acosta AA. *Opuntia-ficus-indica* (Nopal) mucilage as a steel corrosion inhibitor in alkaline media. J Appl Electrochem 2007;37(7):835–41. http://dx.doi.org/10.1007/s10800-007-9319-z.
[14] El-Etre AY. Inhibition of aluminum corrosion using *Opuntia* extract. Corros Sci 2003;45(11):2485–95. http://dx.doi.org/10.1016/S0010-938X(03)00066-0.
[15] Saleh RM, Ismail AA, El Hosary AA. Corrosion inhibition by naturally occurring substances-IX. The effect of the aqueous extracts of some seeds, leaves, fruits and fruit-peels on the corrosion of Al in NaOH. Corros Sci 1983;23(11):1239–41. http://dx.doi.org/10.1016/0010-938X(83)90051-3.
[16] Chandra S, Eklund L. Villarreal RR Use of cactus in mortars and concrete. Cem Concr Res 1998;28(1):41–51. http://dx.doi.org/10.1016/S0008-8846(97)00254-8.
[17] Galán-Marín C, Rivera-Gómez C, Petric J. Clay-based composite stabilized with natural polymer and fibre. Constr Build Mater 2010;24(8):1462–8. http://dx.doi.org/10.1016/j.conbuildmat.2010.01.008.
[18] Mezger TG. The rheology handbook: for users of rotational and oscillatory rheometers. 2nd ed. Hannover: Vincentz Network; 2006.
[19] Schatzmann M, Bezzola GR, Minor H-E, Windhab EJ, Fischer P. Rheometry for large-particulated fluids: analysis of the ball measuring system and comparison to debris flow rheometry. Rheol Acta 2009;48:715–33. http://dx.doi.org/10.1007/s00397-009-0364-x.
[20] Domone P, Hsi-Wen C. Testing of binders for high performance concrete. Cem Concr Res 1997;27(8):1141–7. http://dx.doi.org/10.1016/S0008-8846(97)00107-5.
[21] ASTM Standard C1611/C1611M-09be1. Standard test method for slump flow of self-consolidating concrete. West Conshohocken, PA: ASTM International; 2010.
[22] ASTM Standard C1621/C1621M-09b. Standard test method for passing ability of self-consolidating concrete by J-ring. West Conshohocken, PA: ASTM International; 2009.
[23] ACI Committee 238, Report on measurements of workability and rheology of fresh concrete (ACI 238.1R-08.). Farmington Hills, Michigan: ACI; 2008.
[24] Barnes HA. A handbook of elementary rheology. Institute of Non-Newtonian Fluid Mechanics: University of Wales, Aberystwyth; 2000.
[25] León-Martínez FM, Rodríguez-Ramírez J, Medina-Torres L, Méndez-Lagunas LL, Bernad-Bernad MJ. Effects of drying conditions on the rheological properties of reconstituted mucilage solutions (*Opuntia ficus-indica*). Carbohydr Polym 2011;84(1):439–45. http://dx.doi.org/10.1016/j.carbpol.2010.12.004.
[26] Medina-Torres L, Brito-De La Fuente E, Torrestiana-Sanchez B, Katthain R. Rheological properties of the mucilage gum (*Opuntia ficus-indica*). Food Hydrocolloids 2000;14(5):417–24. http://dx.doi.org/10.1016/S0268-005X(00)00015-1.
[27] Smith AM, Miri T. Alginates in Foods. In: Norton IT, Spyropoulos F, Cox P, editors. Practical food rheology. An interpretive approach. Oxford: Wiley-Blackwell; 2011. doi:10.1002/9781444391060.ch6.
[28] Davis TA, Volesky B, Mucci A. A review of the biochemistry of heavy metal biosorption by brown algae. Water Res 2003;37(18):4311–30. http://dx.doi.org/10.1016/S0043-1354(03)00293-8.
[29] Wallevik JE. Rheological properties of cement paste: thixotropic behavior and structural breakdown. Cem Concr Res 2009;39(1):14–29. http://dx.doi.org/10.1016/j.cemconres.2008.10.001.
[30] Khayat KH, Saric-Coric M, Liotta F. Influence of thixotropy on stability characteristics of cement grout and concrete. ACI Mater J 2002;99(3):234–41.
[31] Feys D, Verhoeven R, De Schutter G. Why is fresh self-compacting concrete shear thickening? Cem Concr Res 2009;39(6):510–23. http://dx.doi.org/10.1016/j.cemconres.2009.03.004.
[32] De Larrard F, Ferraris CF, Sedran T. Fresh concrete: a Herschel–Bulkley material. Mater Struct 1998;31(7):494–8. http://dx.doi.org/10.1007/BF02480474.
[33] Jayasree C, Krishnan JM, Gettu R. Influence of superplasticizer on the non-Newtonian characteristics of cement paste. Mater Struct 2011;44(5):929–42. http://dx.doi.org/10.1617/s11527-010-9677-6.
[34] Roussel N, Lemaître A, Flatt RJ, Coussot P. Steady state flow of cement suspensions: a micromechanical state of the art. Cem Concr Res 2010;40(1):77–84. http://dx.doi.org/10.1016/j.cemconres.2009.08.026.
[35] Leemann A, Winnefeld F. The effect of viscosity modifying agents on mortar and concrete. Cem Concr Compos 2007;29(5):341–9. http://dx.doi.org/10.1016/j.cemconcomp.2007.01.004.
[36] Roussel N, Ovarlez G, Garrault S, Brumaud C. The origins of thixotropy of fresh cement pastes. Cem Concr Res 2012;42(1):148–57. http://dx.doi.org/10.1016/j.cemconres.2011.09.004.
[37] Sonebi M. Rheological properties of grouts with viscosity modifying agents as diutan gum and welan incorporating pulverized fly ash. Cem Concr Res 2006;36(9):1609–18. http://dx.doi.org/10.1016/j.cemconres.2006.05.016.
[38] Cárdenas A, Higuera-Ciapara I, Goycoolea FM. Rheology and aggregation of cactus (*Opuntia ficus-indica*) mucilage in solution. Journal of the Professional Association for Cactus Development 1997;2: 152-159. <http://www.jpacd.org/downloads/Vol2/6_CPUNFAO.pdf>, [accessed 4.09.2012].
[39] Gomez CG, Pérez-Lambrecht MV, Lozano JE. Influence of the extraction-purification conditions on final properties of alginates obtained from Brown algae (*Macrocystis pyrifera*). Int J Biol Macromol 2009;44:365–72. http://dx.doi.org/10.1016/j.ijbiomac.2009.02.005.
[40] Mikanovic N, Sharman J, Jolicoeur C, Khayat K, Pagé M. Compatibility of viscosity-enhancing agents and superplasticizers in cementitious and model systems: Rheology, bleeding, and segregation (SP-262-5). In: Holland TC, Gupta P, Malhotra VM, editors. Ninth ACI international conference on superplasticizers and other chemical admixtures, Seville, 2009. p. 67–84.
[41] Flatt RJ, Larosa D, Roussel N. Linking yield stress measurements: spread test versus Viskomat. Cem Concr Res 2006;36:99–109. http://dx.doi.org/10.1016/j.cemconres.2005.08.001.
[42] Goaszewski J. Correlation between rheology of superplasticized fresh mortars and fresh concretes (SP-262-16). In: Holland TC, Gupta P, Malhotra VM, editors. Ninth ACI international conference on superplasticizers and other chemical admixtures, Seville, 2009. p. 215–236.